IEEE Photonics Journal
An IEEE Photonics Society Publication

Open Access

Real-Time ROADM Filtering Penalty Characterization and Generalized Precompensation for Flexible Grid Networks

(Invited Paper)

Volume 9, Number 3, June 2017

Jie Pan, ***Member, IEEE***
Sorin Tibuleac, ***Senior Member, IEEE***

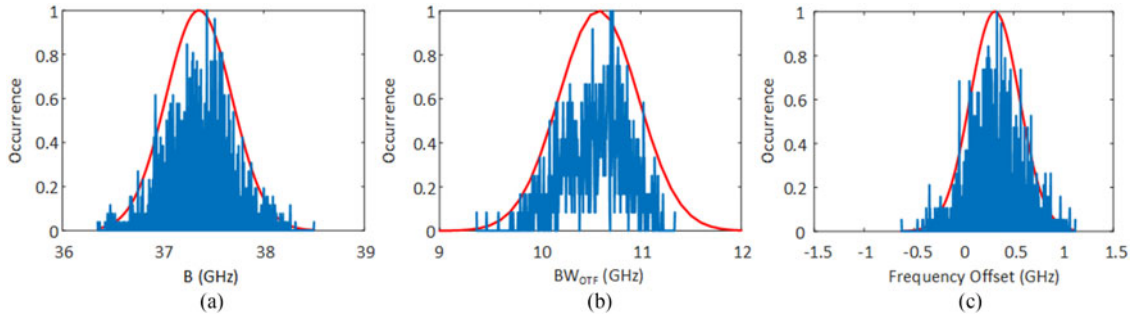

DOI: 10.1109/JPHOT.2017.2699642
1943-0655

Real-Time ROADM Filtering Penalty Characterization and Generalized Precompensation for Flexible Grid Networks

(Invited Paper)

Jie Pan, *Member, IEEE*, and Sorin Tibuleac, *Senior Member, IEEE*

ADVA Optical Networking, Norcross, GA 30092 USA

DOI:10.1109/JPHOT.2017.2699642

Manuscript received April 3, 2017; revised April 24, 2017; accepted April 25, 2017. Date of publication April 28, 2017; date of current version May 15, 2017. Corresponding author: Jie Pan (e-mail: jpan@advaoptical.com).

Abstract: Concatenated filtering is an important impairment in high-spectral density transmission systems enabled by flexible-grid reconfigurable optical add-drop multiplexers (ROADMs). In this paper, an analytical model for wavelength selective switches (WSS) modules is used to determine the statistical distribution of experimentally measured filter shapes and to obtain the cascaded filter characteristics. A generalized approach for filtering penalty assessment is proposed and verified using a commercial 200G 16-quadrature amplitude modulation (16QAM) transponder and WSS modules. A practical method for filter penalty reduction is described, whereby a single, optimized digital pre-equalization filter is used to compensate filtering effects of multiple concatenated WSSs. This pre-equalization of cascaded ROADM filters is demonstrated with a 100G quadrature phase shift keying (QPSK) C-form factor pluggable (CFP) transponder operating on the 37.5-GHz grid, resulting in a doubling of the number of WSSs, which can be supported per link from three to six.

Index Terms: Optical fiber communication, reconfigurable optical add-drop multiplexer (ROADM) filtering, pre-equalization.

1. Introduction

While the current generation of wavelength selective switches (WSSs) is compliant with flexible grid requirements and offers narrow spectral increments of 6.25 GHz to maximize spectral efficiency for 400G or higher superchannel transmission, concatenation of multiple WSS-based reconfigurable optical add-drop multiplexers (ROADMs) can have a severe impact on system performance compared to legacy 100G over 50 GHz grid systems [1]–[3]. So far, cascaded filtering penalties have been quantitatively investigated in terms of the number of concatenated WSSs [4]–[7] or 3 dB bandwidth [4]–[8] for various modulation formats, with different symbol rates and transmission pulse shapes. In such studies, a limited number of WSS shapes is investigated. In a real transmission link, signals may experience a different degree of filtering depending not just on the number of WSS units in the signal path, but depending on different filter shapes corresponding to different WSS designs, or filter shape variation across different ports of a WSS, different wavelengths, or

different attenuation settings as well. Thus, it is critical to find an accurate model for an individual WSS shape to enable detailed analysis on different filter shapes, allowing statistical distributions of the filter parameters to be generated, and accurate WSS-induced transmission penalties to be derived.

An analytical filter model derived from the physics of optical beam propagation within the WSS has been demonstrated to yield a better fit compared to the conventional supergaussian model, wherein the bandwidth of the devices optical transfer function and the bandwidth of the aperture are used to describe a WSS shape [9], [10]. In this work, we use this model to analyze each individual filter shape from different channels, ports and modules of the same WSS design to obtain the statistical distribution of these two aforementioned filter parameters and of the frequency offset. Based on these statistical distributions, simulations are performed to extract the net filter characteristics after the cascade of multiple WSSs. The net filter characteristics are then used in a generalized approach to quantitatively estimate the filtering impact in terms of the OSNR penalty at a reference BER. Specifically, OSNR penalties induced by a Finisar WaveShaper tunable filter loaded with various cascaded filter waveforms are correlated with the OSNR penalties obtained with the cascaded filter bandwidths. Transmission results employing multiple commercial WSS units and a commercial 200G polarization-division multiplexing (PDM)-16 quadrature amplitude modulation (16QAM) transponder are used to verify this relationship experimentally.

It has been shown that filtering penalty constrains the number of ROADM nodes, and hence, the transmission distance in a 37.5 GHz grid network. Various methods have been proposed for mitigating the filtering penalties. For example, the benefit of using a superchannel scheme has been studied [2], where two or more sub-channels are routed as a group to avoid filtering impairments. As the edge sub-channels only experience partial filtering compared to a single sub-channel routing, the filtering impairments can thus be significantly reduced. Other compensation techniques [11]–[16], such as optical spectrum pre-emphasis or digital pre- or post-compensation have been studied. Among them, the digital-to-analog converter (DAC) enabled digital pre-equalization is preferable due to its implementation simplicity, accuracy of spectral pre-emphasis, and its performance benefits. While typical spectral pre-compensation requires a dynamic update of pre-equalization taps to adapt to variations in the routing path, in many practical cases, e.g., a DWDM system with alien wavelengths, the required feedback path from the receiver digital signal processing (DSP) to the transmitter DAC is not available. Therefore, it is desirable to find a generalized pre-equalization filter, which is robust to various routing configurations. In this work, we use a sequence of WSSs with the same filter transmittance to determine a generalized spectral pre-equalization shape for compensating a PDM-quadrature phase shift keying (QPSK) channel transmitted through various number of ROADMs [17]. The resulting performance benefits are verified through real-time measurements, using a commercial CFP 100G PDM-QPSK module [18], which includes a DAC memory that enables a finite tap length pre-equalization filter implementation.

2. WSS Filtering Impariment Assessment

Filtering penalty assessments are critical in ROADM enabled flexible grid networks. While it is unrealistic in network design to characterize filtering penalties arising from all possible combinations of concatenated filter shapes, it is crucial to have an accurate spectral model for an individual filter shape to analyze the distribution of filter characteristics among different WSS modules, and thereby gain insight into the potential outcomes of net filter shapes in ROADM networks.

An analytical model has been proposed [9] based on the physical operation of a WSS designed with free-space optics and applicable to multiple switching technologies, e.g. liquid crystal on Silicon (LCoS) and microelectromechanical system (MEMS). Using this model, a single WSS can be accurately described by the bandwidth of the optical transfer function of the device (BW_{OTF}) and the bandwidth of the aperture (B), as shown in (1) and (2), shown below. Given a measured WSS shape, B is the 6 dB bandwidth while BW_{OTF} can be extracted by taking the derivative of a measured filter spectrum with respect to the frequency [9]. Fig. 1 displays an example for measurement data

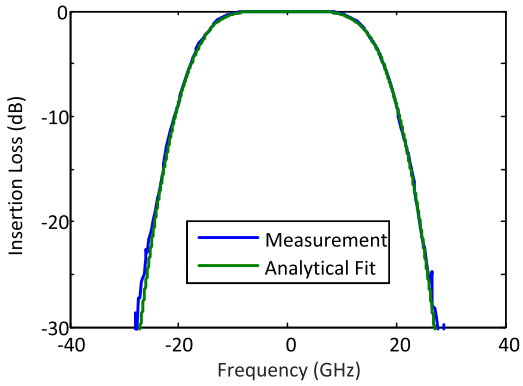

Fig. 1. Measured WSS shape versus analytical fit.

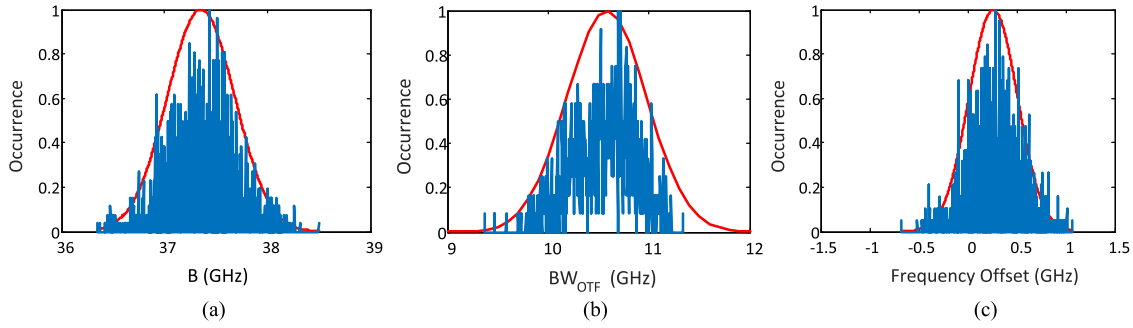

Fig. 2. Statistical distribution of filter shapes measured from different channels and ports of a WSS module. (a) optical 6 dB bandwidth B. (b) Optical transfer function bandwidth BW_{OTF}. (c) Frequency offset.

and the analytical fit.

$$S(f) = \frac{1}{2}\,\sigma\sqrt{2\pi}\left[\mathrm{erf}\left(\frac{\frac{B}{2}-f}{\sqrt{2}\sigma}\right) - \mathrm{erf}\left(\frac{-\frac{B}{2}-f}{\sqrt{2}\sigma}\right)\right] \tag{1}$$

$$\sigma = \frac{BW_{OTF}}{2\sqrt{2\ln 2}}. \tag{2}$$

Using this analytical model, filter shapes of different WSS modules can be statistically analyzed. Fig. 2 shows the data of 1152 filter shapes from different ports and channels of a single 37.5 GHz grid WSS device which is analytically fitted with the statistical distributions. The corresponding B, BW_{OTF}, and frequency offsets show an approximately Gaussian distribution with mean values of 37.4 GHz, 10.6 GHz, and 0.3 GHz, respectively. The statistics of a filter shape can be used to analyze the effect of concatenated filters. Filter shapes which are randomly generated following the distribution in Fig. 2(a) and (b) are cascaded in simulations. Ten thousand runs are performed to obtain a distribution of net filter 6 dB bandwidth, as shown in Fig. 3(a). The bandwidth distribution at other specified levels can be obtained in a similar manner. The frequency offset value is assumed to be zero in this case. Then, B and BW_{OTF} are fixed at mean value to study the frequency offset distribution after cascading different number of filters, as shown in Fig. 3(b). The variance of both the 6 dB bandwidth and the frequency offset reduces with the number of cascaded WSSs. Although the net cascaded filter slope (i.e., sharpness of the edges of the filter transmittance) varies, BW_{OTF} can no longer be used to define the slope because the analytical model only applies to a single WSS. Based on the statistics in Fig. 3, if there exists a simple correlation between the filtering penalty and a net filter bandwidth and if this correlation is moderately affected by the net cascaded

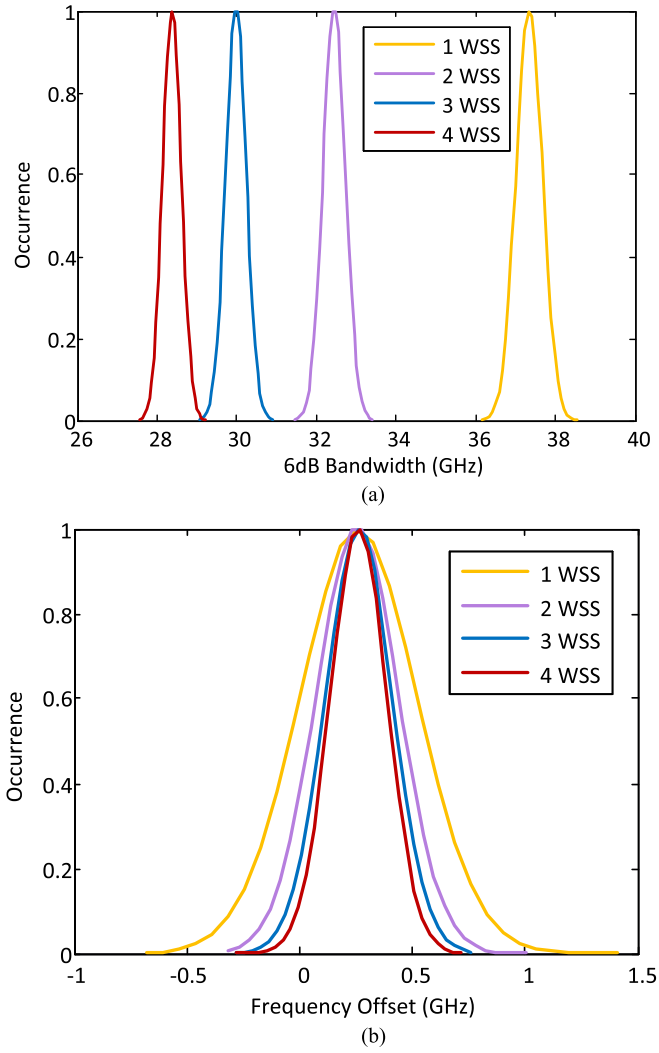

Fig. 3. Statistical distribution of the simulated WSS sequence. (a) 6 dB bandwidth. (b) Frequency offset.

filter slope, then the range of the filtering impairments after transmitting a signal through different number of WSSs can be approximately, yet easily estimated.

In order to establish the correlation between the filtering-induced OSNR degradation and the net filter bandwidth and to evaluate the impact of the net filter slope on this correlation, we study transmission performance subject to net cascaded filter shapes with various bandwidths and slopes. The test signal is generated by a commercial 200G PDM-16QAM transponder with Nyquist root raised cosine roll off 0.2 shaping, 25% FEC and non-differential encoding with a real-time BER measurement. The corresponding symbol rate is 34.17 Gbaud. We first numerically generate 320 net-cascaded filter shapes using individual filters at different B, BW_{OTF}, and frequency offset, and then load the waveforms to a Finisar WaveShaper. Although the measured filter shape deviates from the numerical waveforms, filters with various bandwidth, slope, and frequency offset values are obtained and these measured filter characteristics are used in subsequent analysis. The measured frequency offset is between 0 and 3 GHz. The frequency offset is the signal center frequency based on the 6 dB bandwidth points, measured with respect to the standard ITU grid.

In a second step, the corresponding OSNR penalties of the 320 net-cascaded filter shapes are evaluated versus the filter bandwidths at 0.5 dB, 3 dB and 6 dB. We observe that the net-cascaded

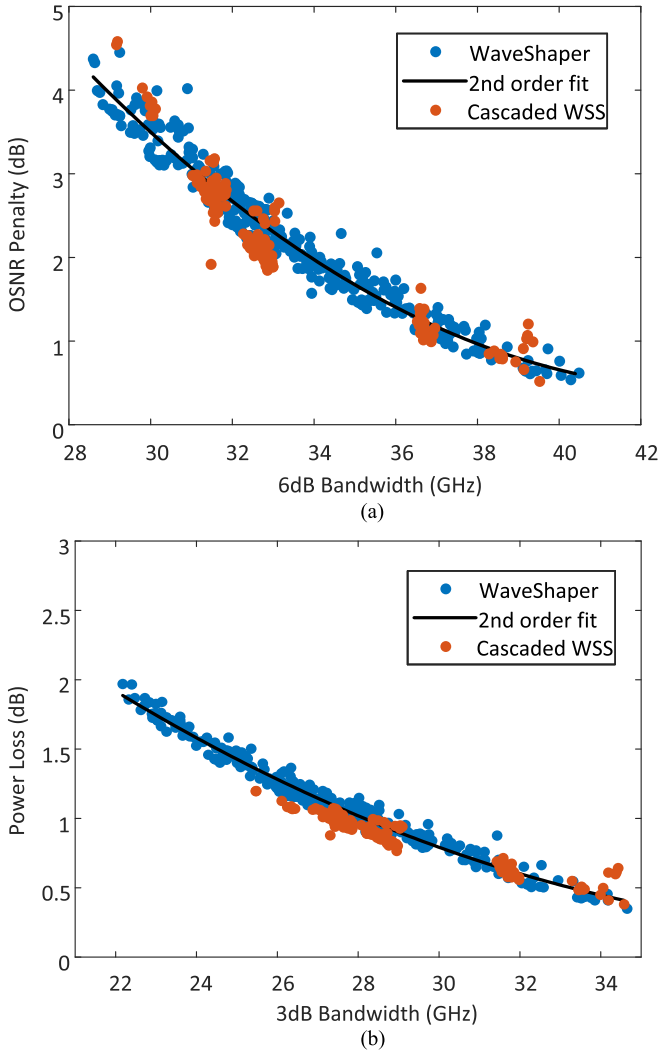

Fig. 4. (a) OSNR penalty versus 6 dB bandwidth at the BER of 2×10^{-2}. (b) Power loss versus 3 dB bandwidth obtained through a Finisar WaveShaper (blue points) or cascaded WSSs (red points).

filter 6 dB bandwidth shows a better correlation with the OSNR penalty compared to the filter bandwidth at other amplitude levels. The OSNR penalty versus the 6 dB bandwidth at BER of 2×10^{-2} is illustrated in Fig. 4(a). In the presence of both frequency offset and filtering slope change, the OSNR penalty at a given 6 dB bandwidth only shows a maximum difference across different slopes and offsets of 0.5 dB at large bandwidths, while the variation is slightly larger at smaller bandwidths. A second order polynomial fitting gives a coefficient of determination of 95.8%, compared to 81.7% and 94.1% for 0.5 dB and 3 dB bandwidth, respectively. We note that OSNR measurement in Fig. 4(a) does not include filtering induced power loss, which is evaluated separately as a function of the filter bandwidth at different levels. In this case, the net filter 3 dB bandwidth better describes the power loss. A second order polynomial fitting delivers a coefficient of determination of 97.8%, compared to 96.6% and 91.5%, corresponding to 0.5 dB and 6 dB bandwidth, respectively.

We further evaluate the filtering penalty and power loss by randomly choosing up to three WSS modules from different vendors and creating transmission paths through different ports set to operate on the 37.5 GHz grid, and then comparing the resulting OSNR penalties to those obtained by the WaveShaper measurements. Both data sets line up well, as shown in Fig. 4. The few outlier

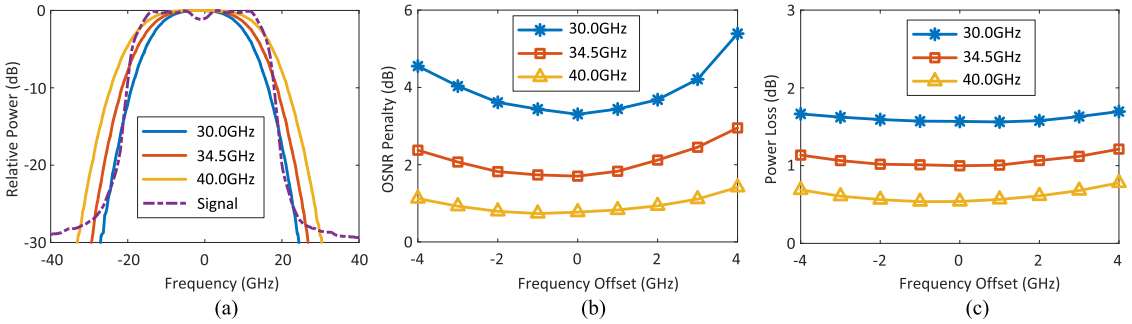

Fig. 5. (a) Spectra of three filter shapes and signal. (b) OSNR penalty versus frequency offset at the BER of 2×10^{-2}. (c) Power loss versus frequency offset for filter shapes at 6 dB bandwidth of 30 GHz, 34.5 GHz, and 40 GHz.

points might be caused by the uncertainties in WSS shape measurement. The OSNR penalty and power loss relations versus the filter bandwidth require recalibration if the transmitted signal spectrum changes. While the tolerable number of concatenated WSSs in a 37.5 GHz flexible grid is limited to only a few WSSs, the number of WSSs traversed in a 50 GHz grid network can exceed twenty, which will create net cascaded filter shapes with sharper slopes. However, hardware limitations in existing tunable filters make it difficult to achieve filter shapes with sharp passband slopes. Thus, the generality of penalty assessment through a single tunable filter for a 50 GHz grid system requires further investigation with large numbers of concatenated WSSs.

Separately, we also evaluate the performance degradation due to frequency offset. This frequency offset denotes the signal frequency shift amount rather than the relative frequency difference between the signal carrier and passband filter center frequency. Three different filter shapes with 6 dB bandwidth of 30 GHz, 34.5 GHz, and 40 GHz are chosen with the corresponding spectra shown in Fig. 5(a) and the OSNR penalty and power loss in Fig. 5(b) and (c), respectively. At 4 GHz frequency offset, the three filter shapes yield maximum OSNR penalty differences relative to the OSNR penalty at zero offset of 2.1 dB, 1.2 dB, and 0.6 dB, respectively. If we only consider the frequency offset at 1 GHz, a realistic value based on our measurements, the OSNR penalty for the three filter shapes drops down to only 0.13 dB, 0.12 dB and 0.06 dB, respectively. The power loss variation versus frequency offset is very small and is negligible within 1 GHz frequency offset range. Therefore, as the frequency offset of the net filter shape becomes less significant for cascaded WSSs, as shown in Fig. 3(b), its impact on system performance becomes negligible in most cases.

3. Pre-Equalization Principles and Benefits

The net filter 6 dB bandwidth decreases significantly with an increasing number of WSS modules in the link, as shown in Fig. 3(a), thereby generating large transmission penalties as indicated in Fig. 4(a). An extension of the WSS sequence traversed by a given signal type subject to a specific flex-grid bandwidth allocation on the WSSs requires appropriate DSP techniques to mitigate the filtering impact. Several pre-equalization filter design methods are available. This filter shape can be obtained using the frequency response of the receiver adaptive equalizer [12], [14] or it can be computed from the received spectrum [7], [13]. The first method is more computationally efficient while the second approach can tolerate more channel estimation noise. However, both algorithms require a feedback path from the receiver DSP to the transmitter DAC. Alternatively, the pre-equalization filter can be calculated using the WSS shapes [6], which is the method used in this work. For a particular link, the pre-equalization filter spectrum is obtained by dividing the desired Nyquist shape by the product of the measured transmittance of cascaded WSSs within the symbol rate and the signal spectrum, as shown in Fig. 6. The pre-equalization filter is then converted to the time domain, quantized, and loaded to the transmitter DAC memory. However, as shown in

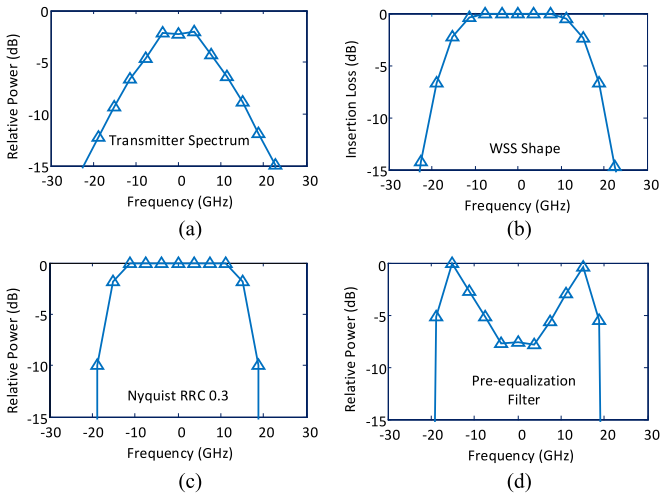

Fig. 6. Spectra of (a) transmitted signal, (b) measured WSS filter, (c) desired Nyquist RRC 0.3, and (d) pre-equalization filter.

TABLE 1

B and BW_{OTF} of the Individual WSS for the Transmission Channel and the 6 dB Bandwidth After Cascading Each WSS

	WSS bandwidth (GHz)	
WSS ID	*Individual*	*Cascaded*
1	36.7/11.0	36.7
2	36.5/10.9	31.8
3	37.0/11.0	29.4
4	36.6/10.7	28.0
5	38.1/10.0	27.3
6	38.2/10.7	26.6

Fig. 2, the filter shapes vary in bandwidth, slope, and frequency offset. Ideally, the pre-equalization filter requires updates in a timely manner and needs recalibration after changes in the number of concatenated WSSs or even after changing WSS ports or channels. Here, we evaluate the possibility of using a generalized pre-equalization filter to compensate different filtering impairments. More specifically, a single pre-equalization shape with a fixed 6 dB bandwidth is used to design a pre-equalization filter and to compensate for the filtering impairments induced by different number of WSSs in a link. Different pre-equalization shapes are evaluated and the optimal shape is identified.

We demonstrate the pre-equalization procedure using a commercial CFP 100G PDM-QPSK transponder with real-time BER measurements. The symbol rate is 30.14 Gbaud and the signal deploys 15% FEC with differential encoding. The transmitter DAC memory is first loaded with an impulse function to extract the transmitted signal spectrum. Up to six WSSs are used in the transmission system. The filter parameters B and BW_{OTF} of the individual WSS for the transmission channel and the measured 6 dB bandwidth after each additional WSS in the sequence are shown in Table I. In the design of the pre-equalization filter, a cascade of three identical filters is used. Four

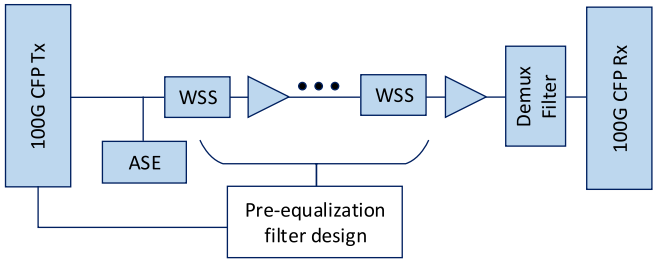

Fig. 7. Block diagram of pre-equalization for ROADM filtering mitigation.

cases are studied, in which the 6 dB bandwidth is set to the values 36 GHz, 37 GHz, 39 GHz, or 41 GHz respectively, and the BW_{OTF} is fixed at 11 GHz. The pre-equalization filter is obtained by concatenating three WSSs modules, and the cascaded 6 dB bandwidths are 28.3 GHz, 29.3 GHz, 31.3 GHz, and 33.3 GHz. The resulting pre-equalization shape is converted to the time domain, quantized, and loaded to the CFP DAC memory, as shown in Fig. 7.

Back-to-back BER versus OSNR results after transmitting the 100G PDM-QPSK signal through different number of WSSs with pre-equalization are plotted in Fig. 8(a). The OSNR measurement in this case does not consider the power loss due to filtering. Using the default CFP shape, the reference required OSNR at the BER of 10^{-2} is 14.0 dB without any WSS in the transmission path. Approximately 0.7 dB and 1 dB OSNR penalty is measured with two and three WSSs in the signal path, and the demodulation fails at four WSS in the transmission path. Therefore, in this particular setup pre-equalization is necessary when extending the transmission distance beyond three WSSs. Theoretically, for an optimal performance, the number of WSSs and WSS shapes used for the pre-equalization filters design should exactly match the actual channel path. However, several drawbacks occur as we maximize the number of WSSs used to pre-compensate the signal. For example, the signal power after modulation becomes lower after pre-equalization for a larger number of WSSs, causing a reduction of the OSNR at the transmitter. Furthermore, as the pre-equalized signal carries more power in the high frequency band, more signal power is carved out from the original signal spectrum after propagating through WSSs, thereby degrading the OSNR. Hence, it is desirable to use the least number of WSSs to design a pre-equalization filter. In this study, a pre-equalization filter design based on three WSSs is used to compensate the filtering penalty caused by three to six WSSs.

Different pre-equalization design options are compared in Fig. 8(a). The dashed line is the pre-equalization reference, where the measured transmittance of the first three WSSs is used to design the pre-equalization filter. The others are designed using three identical cascaded WSS shapes with different net 6 dB bandwidths. The reference curve falls between the curves for B of 36 GHz and 37 GHz curves. For each case, the optimal performance occurs after transmission through a different number of WSSs. This is explained by the increased filtering effect compensated by the pre-equalization for lower filter bandwidth. If the WSS bandwidth in the design is too high, it will lead to inadequate pre-emphasis, which explains the BER failure at six WSSs for B equals 41 GHz. With decrease in bandwidth below the optimum value, the pre-equalization benefit also decreases due to the signal power loss from filtering, as shown in Fig. 8(b). As the filter shape bandwidth decreases, the power loss becomes more significant due to the enhanced power of the pre-compensated signal at high frequencies. This also explains the results illustrated in Fig. 8(a) where the pre-equalization filter designed with larger bandwidth shows more benefit. Therefore, in general, taking a larger WSS bandwidth into consideration is preferred for pre-equalization for systems where performance is a major concern. A smaller WSS bandwidth is used to maximize number of WSS in the transmission link.

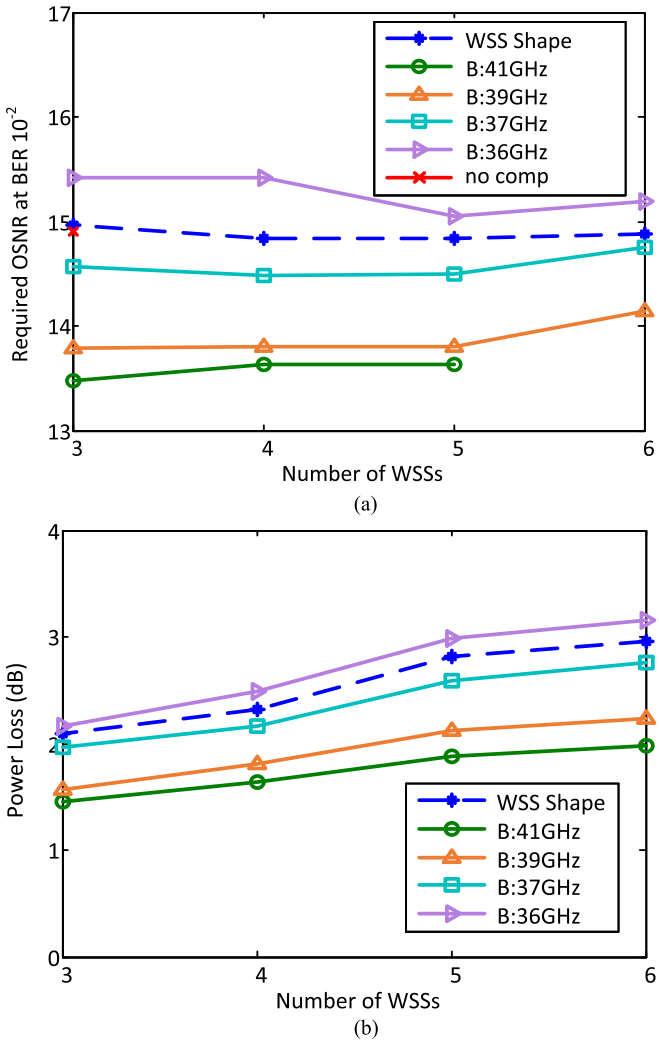

Fig. 8. (a) Required OSNR at the BER of 10^{-2} with different WSS filter bandwidths used for pre-equalization. (b) Signal power variation with different WSS filter bandwidths used for pre-equalization.

4. Conclusion

In this work, we use an analytical model to study the statistical distribution of concatenated filter shapes. The measured OSNR penalty has been found to correlate well with the 6 dB bandwidth for various filter shapes required for a 37.5 GHz grid network, and the filter induced power loss is well described by the 3 dB bandwidth. We have demonstrated compensation of the filtering effect of flexible grid ROADMs operating on the 37.5 GHz grid by implementing pre-equalization in a commercial CFP transponder. Instead of updating the pre-equalization filter for different link configurations, we present a simpler alternative whereby a single pre-equalization filter compensates filtering effects for all realistic cases. This approach has enabled an increase in the number of WSSs supported by the 37.5 GHz spaced 100G QPSK signal from three to six. While the number of WSS in the sequence is still too low to cover all network applications, this enhancement in add/drop functionality does substantially increase the range of applicability of 37.5 GHz-grid DWDM systems in regional networks using broadcast-and-select ROADMs.

References

[1] A. Morea, J. Renaudier, T. Zami, A. Ghazisaeidi, and O. Bertran-Pardo, "Throughput comparison between 50-GHz and 37.5-GHz grid transparent networks," *IEEE/OSA J. Opt. Commun. Netw.*, vol. 7, no. 2, pp. A293–A300, Feb. 2015.

[2] J. Pan and S. Tibuleac, "Filtering and crosstalk penalties for PDM-8QAM/16QAM super-channels in DWDM networks using broadcast-and-select and route-and-select ROADMs," in *Proc. Opt. Fiber Commun. Conf. Exhib.*, 2016, Paper W2A.49.

[3] A. Ghazisaeidi *et al.*, "Impact of tight optical filtering on the performance of 28 Gbaud nyquist-WDM PDM-8QAM over 37.5 GHz grid," in *Proc. Opt. Fiber Commun. Conf. Expo. Nat. Fiber Optic Eng. Conf.*, 2013, Paper OTu3B.6.

[4] F. Heismann, "System requirements for WSS filter shape in cascaded ROADM networks," in *Proc. Opt. Fiber Commun. Conf. Expo. Nat. Fiber Optic Eng. Conf.*, 2010, Paper OThR1.

[5] E. B. B. Pal, L. Zong, and H. P. Sardesai, "Statistical method for ROADM cascade penalty," in *Proc. Opt. Fiber Commun. Conf. Expo. Nat. Fiber Optic Eng. Conf.*, 2010, Paper NThF2.

[6] T. Rahman *et al.*, "On the mitigation of optical filtering penalties originating from ROADM cascade," *IEEE Photon. Technol. Lett.*, vol. 26, no. 2, pp. 154–157, Jan. 2014.

[7] X. Zhou *et al.*, "On the capacity improvement achieved by bandwidth-variable transceivers in meshed optical networks with cascaded ROADMs," *Opt. Exp.*, vol. 25, no. 5, pp. 4773–4782, 2017.

[8] D. Rafique and A. D. Ellis, "Nonlinear and ROADM induced penalties in 28 Gbaud dynamic optical mesh networks employing electronic signal processing," *Opt. Exp.*, vol. 19, no. 18, pp. 16 739–16 748, 2011.

[9] C. Pulikkaseril, L. A. Stewart, M. A. F. Roelens, G. W. Baxter, S. Poole, and S. Frisken, "Spectral modeling of channel band shapes in wavelength selective switches," *Opt. Exp.*, vol. 19, pp. 8458–8470, 2011.

[10] J. Pan, C. Pulikkaseril, L. Stewart, and S. Tibuleac, "Comparison of ROADM filter shape models for accurate transmission penalty assessment," in *Proc. IEEE Photon. Conf.*, 2016, pp. 550–551.

[11] Z. Dong, X. Li, J. Yu, and N. Chi, "6×144-Gb/s nyquist-WDM PDM-64QAM generation and transmission on a 12-GHz WDM grid equipped with nyquist-band pre-equalization," *J. Lightw. Technol.*, vol. 30, no. 23, pp. 3687–3692, 2012.

[12] J. Zhang, H. C. Chien, Y. Xia, Y. Chen, and J. Xiao, "A novel adaptive digital pre-equalization scheme for bandwidth limited optical coherent system with DAC for signal generation," in *Proc. Opt. Fiber Commun. Conf. Exhib.*, 2014, Paper W3K.4.

[13] J. Pan, P. Isautier, J. S. Langston, and S. E. Ralph, "DAC enabled frequency domain pre-shaper design for nyquist signaling," in *Proc. Adv. Photon. Commun.*, 2014, Paper SM3E.2.

[14] Z. Jia, H. C. Chien, J. Zhang, Z. Dong, and Y. Cai, "Performance analysis of pre- and post-compensation for bandwidth-constrained signal in high-spectral-efficiency optical coherent systems," in *Proc. Opt. Fiber Commun. Conf. Exhib.*, 2014, Paper W3K.3.

[15] R. Schmogrow *et al.*, "Pulse-shaping with digital, electrical, and optical filters-a comparison," *J. Lightw. Technol.*, vol. 31, no. 15, pp. 2570–2577, 2013.

[16] O. Bertran-Pardo, T. Zami, B. Lavigne, and M. L. Monnier, "Spectral engineering technique to mitigate 37.5-GHz filter-cascade penalty with real-time 32-GBaud PDM-16QAM," in *Proc. Opt. Fiber Commun. Conf. Exhib.*, 2015, Paper M3A.3.

[17] J. Pan and S. Tibuleac, "Real-time pre-compensation of ROADM filtering using a generalized pre-emphasis filter," in *Proc. IEEE Photon. Conf.*, 2016, pp. 548–549.

[18] Y. Loussouarn, M. Song, E. Pincemin, G. Miller, A. Gibbemeyer, and B. Mikkelsen, "100 Gbps coherent digital CFP interface for short reach, regional, and ultra long-haul optical communications," in *Proc. Eur. Conf. Opt. Commun.*, 2015, pp. 1–3.